Computational Investigation of Flow Control over Wings

Panagiotis S. Vavilis, John A. Ekaterinaris

Department of Mechanical and Aerospace Engineering,

University of Patras, and FORTH/IACM Heraklion, Crete, Greece.

Abstract. Passive and active flow control concepts for control of flow separation over wings are simulated numerically. Passive flow control is applied with small delta-wing-type vortex generators that are submerged in the boundary layer. A parametric study of the vortex generators arrangement and their orientation with respect to the free stream is carried out. For the same location of the vortex generators, active flow control with steady and pulsating jets is applied to suppress separated flow and increase the aerodynamic performance of the wing. The effectiveness of each flow control mechanism is assessed.

Key words: passive flow control, active flow control.

1. Introduction

Establishment of active or passive control of flow separation over aircraft wings, helicopter, or wind-turbine rotor blades, has been a continuous effort of experimental and theoretical investigations for the past decades. An extensive review of techniques employed for the manipulation of flow separation was given by Gad-el-Hak [1]. Numerous experimental investigations [2, 3, 4, 5] have tested passive and active flow control concepts. Among them, active control of separated flows with pulsating jets [2, 3, 4] yielded very encouraging results. It was also demonstrated [5] that oscillatory blowing is more effective than steady blowing in controlling boundary-layer separation and improving dynamic airfoil performance by eliminating large excursions in lift, drag, and pitching moment. Recent reviews on flow control [6, 7, 8] give a full account of past and recent efforts for flow control and a comprehensive presentation of various flow control mechanisms.

Despite the effectiveness of innovative, active flow control techniques, passive flow control with vortex generators (VG's) [9] is still widely used in practice for both transport aircraft wings and wind-turbine blades in order to enhance aerodynamic performance and control flow separation. Among the VG configurations used [9], the most widely known are the vane-type, wheeler-type or simple delta-wing-type. Vane-type VG's are rectangular blades which are mounted on the wing surface in co-rotating or counter-rotating arrangement. They energize the wing boundary layer with the strong tip vortex they generate. The main parameters determining the strength of the tip vortex are the incidence angle and the chord length. The wheeler and delta-wing VG's are essentially delta planforms with large sweep angle $\Lambda > 60^o$

deg., which are mounded on the surface of the wind-turbine rotor blade or the aircraft wings (see Fig. 1) at an incidence angle ($15^o < \gamma < 20^o$) with respect to the incoming boundary-layer flow. The main parameters determining the strength of the helical vortex generated by a delta-wing-type VG, are shown on the left of Fig. 1. Furthermore, these VG's can be placed on the wing surface either in counter-rotating (antisymmetric) or co-rotating (periodic) arrangement as shown on the right of Fig. 1. The distance between the VG's is another flow control parameter. The tip vortex of vane type VG's, or the helical vortex generated by the delta wing transports momentum from the edge of the boundary layer and the free stream to the near wall region, it energizes the boundary layer, and makes possible for the flow downstream of the VG to be able to withstand adverse pressure gradients without separation. Flow reattachment with vortex generators is achieved, however, at the expense of an increase in drag.

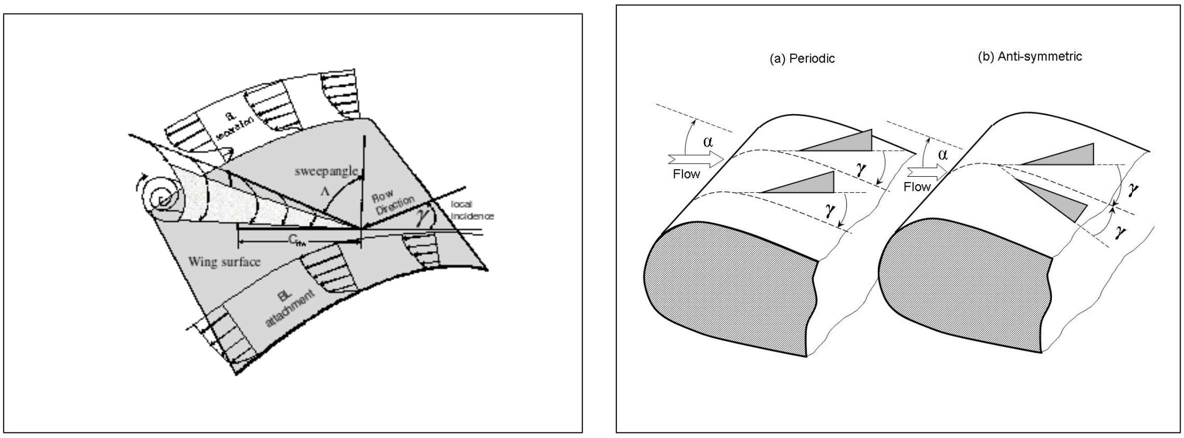

Figure 1. Schematic of a delta wing type vortex generator, and VG arrangement.

Active flow control actuators appear to be promising for effective control of flow separation and performance enhancement in a wide range of operation conditions without severe drag penalty. Effective boundary layer control of the flow over airfoils was demonstrated in experiments with pulsating jets [4, 5]. Codard and Stanislas [10] recently presented a comparative experimental investigation of the effect of VG's and pneumatic flow control with jets emanating from slots arranged in a similar manner to vortex generators.

Simulation of VG's passive flow control, or pneumatic flow control for high Reynolds number $Re_c > 10^6$ turbulent wing flows could be accomplished either by the numerical solution of the Reynolds-averaged Navier-Stokes (RANS) equations or by large eddy simulations (LES). The full interaction of flow control devices with the boundary layer and capturing of the details of instability and receptivity mechanisms triggered by flow control can only be obtained with LES. However, we concluded that LES of the high Reynolds number flow fields generated by passive and active flow controls on realistic configurations, such as wings, are still beyond the capabilities of available computing resources.

Numerical prediction of the beneficial effects of flow control on airfoils reported in experimental studies was the subject of several investigations [11, 12] and references therein. Most numerical investigations with pulsating jets were essentially based on the assumption of two-dimensional flows, even though three-dimensionality is an essential feature of pneumatic flow control mechanisms. In the numerical studies of VG flow control, the tree-dimensional flow character cannot be ignored or simplified. The numerical and experimental work of Ref.[13] is one of the few recent investigations that addressed VG flow control and performed RANS for full configurations of VG's on wings. In this paper, low speed flow control with VG's and steady or pulsating jets exiting from slots, which are oriented at an angle with respect to the free stream, is considered. The three-dimensional incompressible flow field they generate over stationary wings is simulated with unsteady RANS. The unstructured flow solver FLUENT (http://www.fluent.com/software/fluent/) is used for the numerical solution. High mesh density is required to resolve the essential details of the VG flow field. The jet flow is imposed as a boundary condition on the blade surface.

2. Flow Control Device Parameters

The main vortex generator parameters (see Fig. 1) are the sweep angle, Λ, of the delta wing and the chord length c_{dw}. The chord length c_{dw} and sweep angle Λ are not independent since the span (hight) of the VG, s, must be limited to values $s = c_{\mathrm{dw}} \tan\Lambda$ that yield VG's submerged in the boundary layer, $0.25\delta < s < 0.5\delta$, as suggested in the experimental investigations summarized in Ref. [9]. It was also demonstrated in experiments [8] that the important parameters for airfoil flow control with pulsating jets are (i) the reduced excitation frequency, $F^{+} = cf_J/U$ where c is the airfoil chord, and f_J is the jet pulsation frequency and (ii) the oscillatory blowing momentum coefficient, $C_\mu = \langle J\rangle/cq$, where $q = 0.5\rho U^2$, $\langle J\rangle$ is the oscillatory momentum, $\langle J\rangle = \rho V_J^2 H_J, H_J = H\sin\theta_J$ when the jet exits at an angle θ_J with respect to the surface, and V_J is the oscillatory jet exit velocity. In this investigation, we do not perform optimization of flow control device parameters but simply demonstrate that unsteady RANS solutions can be used to predict performance enhancements resulting from the application of passive and active flow control.

3. Results

The objective of this work is to demonstrate that the effect of passive flow control with VG's over the realistic configurations and flow conditions, which were investigated experimentally [14], can be assessed using RANS simulations and a general purpose solver, such as FLUENT. Numerical simulation of transonic flow control over a wing using RANS were recently carried out [13], and LES for a VG model problem were presented. The resolution demands for RANS are quite large because high mesh density is needed especially at the region of the VG and downstream. These requirements can be most readily met by a mixed type of mesh. The requirements of LES for VG and pneumatic flow control over wings at $R_e > 10^6$ exceed the available resources, while RANS can be used to simulate these even at flight conditions.

3.1. Flow without control

Initially, steady flow over the wing with NACA-63-415 sections without vortex generators was computed at the same flow conditions as the experiment [14], $R_e = 1 \times 10^6$ for incidences $\alpha = 8^o$, $\alpha = 14^o$, and $\alpha = 18^o$. Fully turbulent flow was assumed and the one-equation Spalard-Allmaras turbulence model [15] was used to compute the turbulent eddy viscosity. For the 2D computations, approximately 30000 cells were used, and 3D results were obtained with ten planes in the spanwise direction. Good agreement with the measurements for smooth wing was found for both the 2D and 3D computations. Numerical solutions on much finer meshes, up to four times the density of the 30000 cell mesh, did not improve the agreement with the experiment. The computed flow fields for $\alpha = 14$ and 18 deg. indicated a large region of flow separation approximately downstream of the $x/c = 0.5$ chord location.

3.2. Flow Control with VG's and Jets

The VG we used for the simulations had the same geometry as in the experiment with a sweep angle $\Lambda = 75^o$, chord length $c_{\mathrm{dw}} = 0.01c$, and height (span) $s = c_{\mathrm{dw}} \tan 15^o = 0.0026c$. The VG was mounted on the wing at $x/c = 0.1$ at an incidence $\gamma = 17.7^o$. Numerical solutions were computed with the VG mounted on the wing for the same incompressible flow conditions as the experiment [14], $R_e = 10^6$ at $\alpha = 8^o$, $\alpha = 14^o$, and $\alpha = 18^o$. The flow was again assumed fully turbulent. For the computations, a mixed-type structured/unstructured mesh was used. Grid converged 3D numerical solutions for the clean wing (without flow control devices) were obtained with approximately 3×10^5 elements. Simulations with flow control required much finer resolution at the location of the VG or the jet and downstream. Several grid refinement studies were performed using meshes containing from 10^6 up to 2.5×10^6 elements. The computed results at the highest incidence, $\alpha = 18^o$, obtained with a mesh of approximately 2.5×10^6 elements were the same with the results obtained with the 2.0×10^6 element mesh. Therefore the mesh with approximately 2.0×10^6 elements was used for all computations because it was concluded that it provides sufficient resolution for accurate capturing of both the near wall viscous flow of the wing and the VG, and the proper convection of the vortical flow structures generated by the VG or the surface jet. All meshes levels contained a canonical, high-resolution mesh box behind the trailing edge of the vortex. This mesh extended over the wing for several VG chord lengths in order to provide the necessary resolution for the convection of the helical vortex generated by the VG delta-wing section, with minimal numerical diffusion. The spanwise and normal to the wall mesh resolution was however progressively reduced towards the trailing edge and outside the boundary layer, respectively.
Most numerical simulations were carried out for a wing with vortex generators placed on its surface with an anti-symmetric or counter-rotating arrangement which was found more effective in the experiments [9, 10]. The less effective periodic or co-rotating VG arrangement was also considered. For this arrangement, two VG's must be included in the simulations and approximately 4.0×10^6 elements are required. Periodicity in the spanwise direction is imposed. For the anti-symmetric arrangement, at the spanwise boundaries of the computational domain symmetry conditions are imposed and only one VG or jet slot is needed.

Comparisons of the the experimental measurements at $\alpha = 8^o$, $\alpha = 14^o$, and $\alpha = 18^o$ with the computed surface pressure coefficient distribution obtained for anti-symmetric VG arrangement is shown in Figs. 2, 3, and 4. For reference, the measured surface pressure coefficients without VC's are also included in these figures. Clearly, the effect of vortex generators is captured correctly with the mesh density used for the computations. The agreement with the experiment at low incidence of $\alpha = 8^o$ is very good. It also appears that the flow attachment predicted by the experiment [14] is well captured by the computations at $\alpha = 14^o$, and $\alpha = 18^o$. For the incidence, $\alpha = 14^o$, the effect of a VG with double size was also simulated. The computed solution of Fig. 3 demonstrated that separation was completely eliminated with the larger VG.

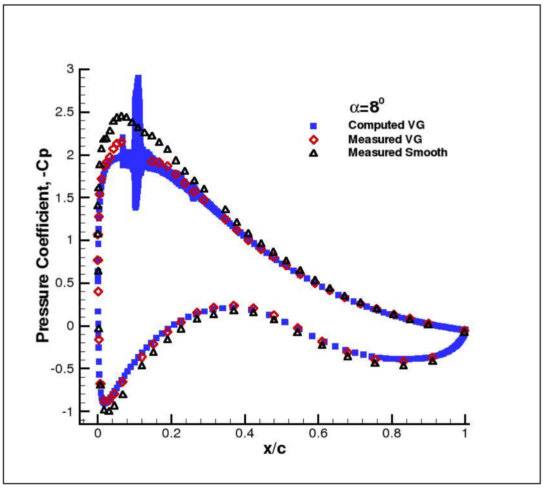

Figure 2. Comparison of the computed and measured surface pressure confident at $\alpha = 8$ deg. with VG flow control.

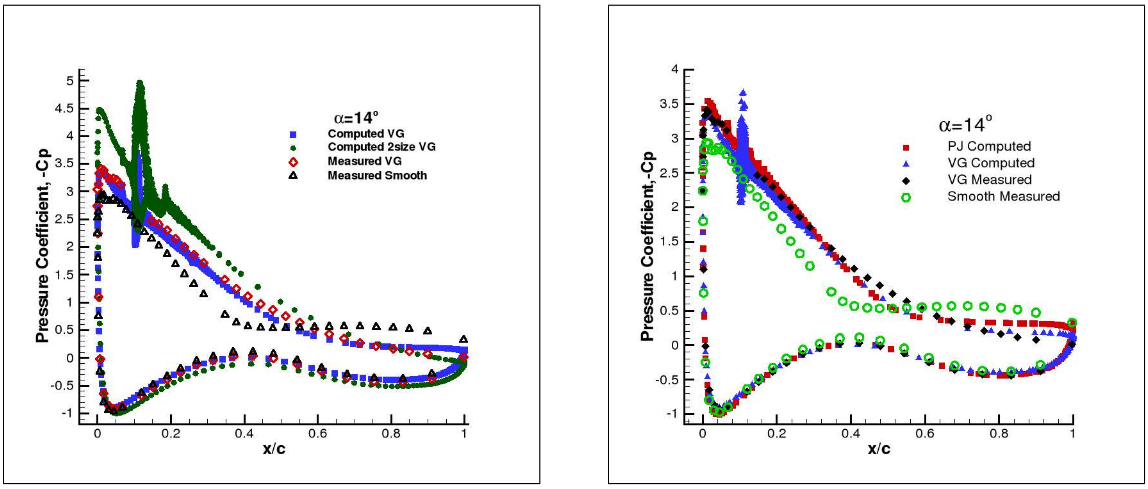

Figure 3. Comparison of the computed and measured surface pressure confident at $\alpha = 14$ deg. with VG and pulsating jet control

Flow control simulation with steady and pulsating jets emanating from slots with

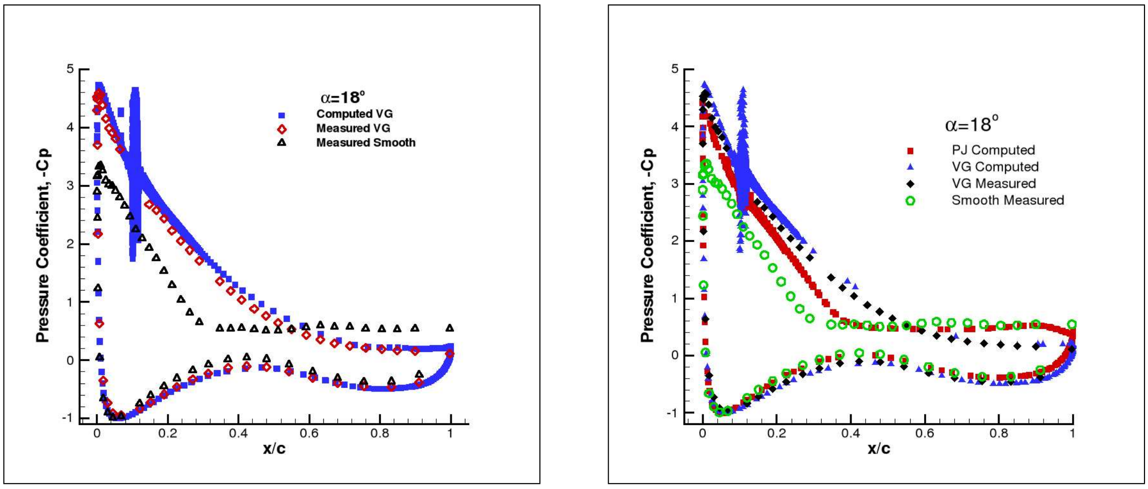

Figure 4. Comparison of the computed and measured surface pressure confident at $\alpha = 18$ deg. with VG and pulsating jet control

the same size and location as the VG's were also carried out. In these tests, the jet slot had a rectangular shape with length $H_J = 0.0166$ and width $t_J = 0.00166$. The slot was also oriented at the same baseline incidence angle as the VG, e.g. $\gamma = 17.7^o$. The jet exited from the slot at an angle $\theta_J = 30^o$ deg. with respect to the wing surface and the jets slots were considered in anti-symmetric arrangement. Flow control with a steady jet with $C_\mu = 0.2133$ was considered first. From the inspection of the computed solutions, it was found that the interaction of the inclined steady jet with the oncoming near wall flow caused a spiraling flow pattern analogous to the flow pattern (but less intense) that was caused by the vortex generator, which created the distinct spiral vortex characterizing the flow over the VG mounted on the wing surface. Flow control with a pulsating jet with $C_\mu = 0.1066$ and frequency parameter $F^+ = 0.5$ was considered next. Again similar interaction of the pulsating jet and the near wall flow was observed.

The computed results for pneumatic flow control simulations are summarized in Figs. 3 and 4. The comparison of the computed surface pressure coefficients at $\alpha = 14^o$ deg. (see Fig. 3) shows that both steady and pulsating jet flow control is effective in suppressing flow separation. Flow control with steady jet was not effective at larger incidence $\alpha = 18$ deg. and the computed pressure distribution with pulsating jet flow control shows that the flow separation could not be suppressed at the same extent as with the VG. Previous investigations [11, 12] indicated that the location of the pneumatic flow control over the wing surface plays an important role on flow control effectiveness. The frequency parameter, exit angle, θ_J, and jet flow speed or C_μ also determine the effectiveness of the flow control. For the present arrangement, the orientation, Λ, of the jet slot and the spanwise distance of the slots could also play a role on the effectiveness of the pneumatic flow control. In the present work, parametric studies with variation of these parameters were not carried out. It was concluded that pneumatic flow control was less effective at least for the flow control parameters considered in this investigation. Identification of the optimal streamwise location and strength (outflow speed or C_μ) of the jet in order to achieve more effective flow control at various incidences could be obtained with parametric studies.

3.3. Effect of Flow Control the Wing Boundary Layer

The effect of anti-symmetric VG arrangement on the boundary layer flow structure is shown in Fig. 5 for the flow at $\alpha = 14^o$. The computed solution is for the baseline configuration ($\Lambda = 75^o, \gamma = 17.7^o$). The computed velocity profiles over the clean wing surface and the wing with VG are compared in Fig. 5 for the region behind the VG and the region where flow separation starts on the clean wing. The alteration of the velocity distribution at the VG location is evident (see Fig. 5 left).

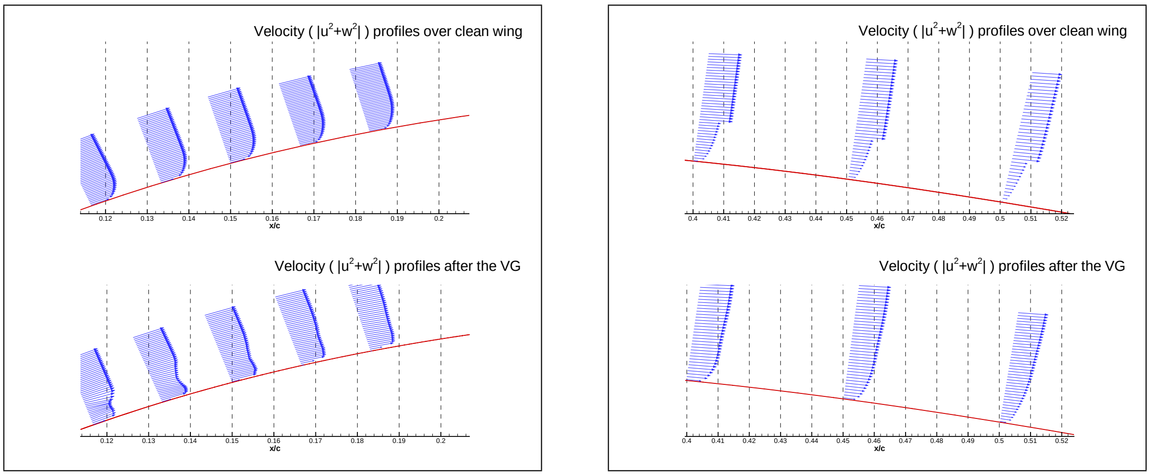

Figure 5. Comparison of the computed near wall flow at $\alpha = 14$ deg. for clean wing and flow control with VG's.

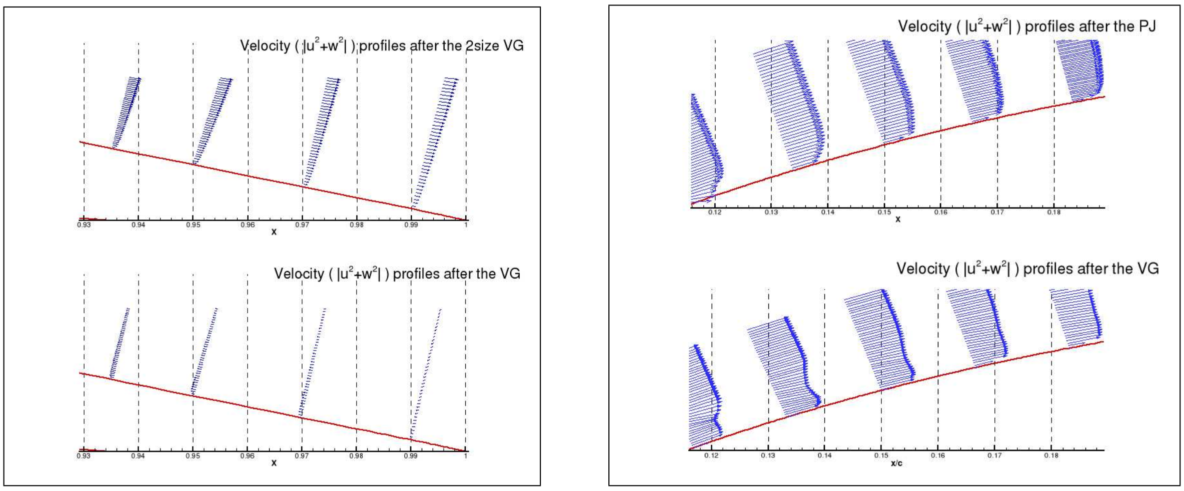

Figure 6. Computed near wall flow at $\alpha = 14$ deg. for large VG and pulsating jet flow control.

A jet like velocity distribution develops downstream the VG and causes transport of fluid to the near wall region. As a result, the kinetic energy within the boundary layer is increased and as this energy is transported downstream the near wall flow over the wing becomes less susceptible to flow separation. It appears, however, that the modification of the boundary layer due to the presence of the VG is associated with an increase in viscous drag. The velocity profiles also remain fuller for several

VG chord lengths downstream. The alteration of the velocity profiles is also clear further downstream. Fig. 5 on the right shows a comparison of the velocity profiles before the location where separation occurs on the clean wing. Clearly, the velocity profiles for the wing with the VG remain fuller and they are able to withstand flow separation that is caused by the adverse pressure gradient on the clean wing.
The effect of a VG with double high (span s) compared to the baseline VG with $s = 0.0026c$ was also tested. It was shown in Fig. 3 that a longer ($c_{\mathrm{dw}} = 0.02, s = 0.0052$) VG is more effective than the baseline VG which is submerged in the near wall region of the wing boundary layer. The comparison of the computed velocity profiles at the trailing edge region (see Fig. 6 on the left) shows that the larger size VG results in fully attached flow. The velocity distribution near the pulsating jet (shown at the peak of the cycle) of Fig. 6 on the right indicates that the alterations of near wall flow caused by the pulsating jet are similar (see Fig. 5 right) to the ones observed for the VG.
It is concluded that high resolution RNAS simulations can be used for fairly accurate predictions of the VG effects over wings at realistic high Reynolds number flow conditions. In addition, simulations can be used to carry out parametric studies of the effects of various VG parameters such as orientation and VG height within the boundary layer. Performance optimization of the VG with variation of these parameters does not appear straight forward because grid motion is difficult and re-meshing of every new configuration is quite time consuming. In addition, LES for wings and VG's currently do not appear to be very practical.

3.4. Parametric Studies of VG Flow Control

The performance of vortex generators is affected by many parameters. The main parameters that determine the effectiveness of the vortex generator are its shape (sweep angle Λ shown in the sketch of Fig. 1). The main function of vortex generators is to enhance wing performance by keeping the flow attached over the wing. It is clear that the shape, the location, and the incidence, and the separation distance of the VG's can be chosen in a way which maximizes its effectiveness. However vortex generator effectiveness optimization with CFD is a formidable task even for the most sophisticated modern optimization techniques [16] that are based on adjoint methods, because generation of the grid at the VG region is not trivial, and grid movement cannot be easily performed for grids with very small elements. Therefore here only a simple sensitivity study of the parameters that determine the performance of vortex generators is attempted. Similar to Ref. [13] this sensitivity study is carried out for a model problem that encompasses all relevant flow features of the wing/vortex generator system. The model problem is a vortex generator in the turbulent boundary layer over a flat plate. The flat plate turbulent boundary layer has the same Reynolds number as the boundary layer on the wing.
Delta wings at high incidence develop helical vortices that can propagate to long distances beyond the trailing edge. The helical vortices of VG's produce enhanced mixing close to the wing surface and help the boundary layer to withstand flow separation caused by the adverse pressure gradient at the wing suction side. The leeward side structure of the flow field over the VG was investigated with several simulations. It was found that the periodic VG arrangement could offer some benefit because the signature of the leading edge vortices from adjacent VG's in the periodic

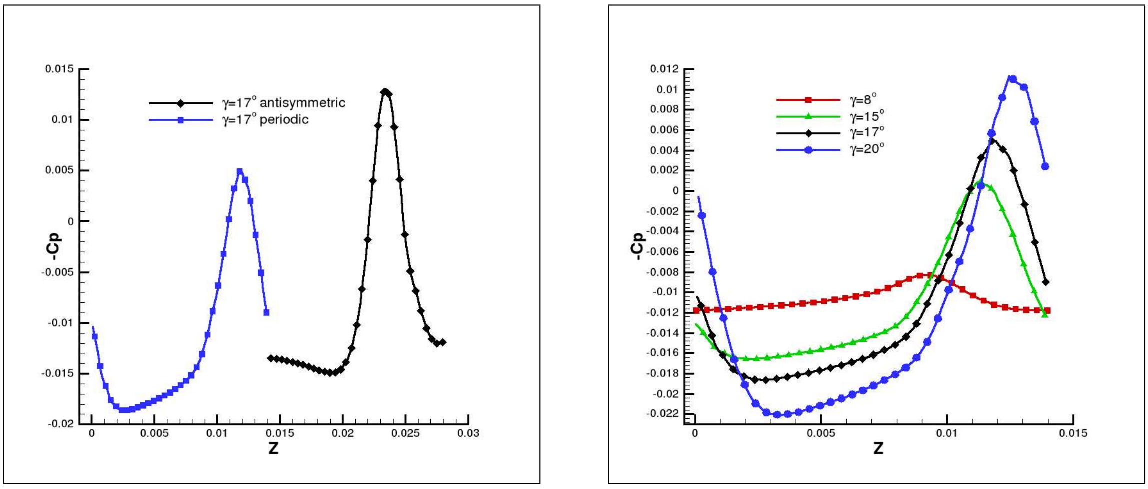

Figure 7. Comparison of the computed and measured surface pressure confident at $\alpha = 18$ deg.

VG array can affect the flow on the wing boundary layer downstream from each VG trailing edge.

It is difficult, however, to conclude from the inspection of the computed flow fields which arrangement is more suitable for the suppression of flow separation. In addition, the effectiveness of the periodic arrangement depends on the VG separation distance. The effect of each VG arrangement was judged by comparing the surface pressure variations caused by the VG's placed in periodic and anti-symmetric arrangements. It is was concluded that the anti-symmetric arrangement causes larger suction after the VG. Therefore it is expected, due to the stronger vortex, that larger momentum transfer from the free stream to the near wall flow could be archived with this arrangement. On the other hand, the periodic VG arrangement causes pressure variations for a larger extent behind the vortex because the leading edge vortices generated from the entire array are present. It is therefore reasonable that the net effect of the periodic and the anti-symmetric arrangement on flow control assessed by the surface pressure distribution of the wing were found quite similar for small separation distance. A quantitative comparison of the effect of the VG arrangement is shown in Fig. 7 with the computed surface pressure coefficient distributions on the wing surface behind the VG's obtained for anti-symmetric and periodic arrangements. It is evident that the suction of the vortex generated by the anti-symmetric arrangement is over the double from the suction produced by the periodic VG arrangement.

The effect of the VG incidence angle, γ, with respect to the free stream was examined next. Only the anti-symmetric VG configuration was considered in this test. A comparison of the computed pressure coefficient distributions on the wing surface behind the VG obtained at difference incidence indicated that the increase of the VG incidence angle γ could increase significantly its effectiveness since lager suction enhances the capability to transfer higher momentum fluid to the near wall region. Therefore the VG incidence angle may be changed dynamically to increase the envelope of its effectiveness.

4. Conclusions

High resolution RANS computations were carried out for passive flow control with VG's and pneumatic flow control. Good agreement with the measurements is obtained provided that high grid resolution is used. Active pneumatic flow control is applied at the same location where the VG's were mounted on the wing. It was found that passive flow control with VG reduces flow separation more effectively than pneumatic flow control.

References

[1] Gad-el-Hak, M. and Bushnell, D. M. Separation Control: Review. *Journal of Fluids Engineering*, 113 (5): 5-30, 1991.

[2] Seifert, A., Bachar, T., Koss, D., Shepshelovich, M., and Wygnanski, I. Oscillatory Blowing a Tool to Delay Boundary-Layer Separation, *AIAA Journal*, 31(11): 2052 - 2060, 1993.

[3] Seifert A., Darabi, A., and Wygnanski I. Delay of Airfoil Stall by Periodic Excitation. *Journal of Aircraft*, 33(4): 691 - 698, 1996.

[4] Seifert, A. and Pack, L. G. Oscillatory Control of Separation at High Reynolds Numbers. *AIAA Journal*, 37(9): 1062-1079, 1999.

[5] Weaver, D., McAllister, K. W., and Tso, J. Suppression of Dynamic Stall by Steady and Pulsed Upper - Surface Blowing. AIAA Paper 98-2413, 1998.

[6] Hwang, D. Review of Research in the Concept of the Microblowing Technique for Turbulent Skin Friction Reduction. *Progress in Aerospace Sciences*, 40(8): 559-575, 2004.

[7] Collis, S. S., Joslin, R. D., Seifert, A., and Theofilis, V. Issues in Active Control: Theory, Control, Simulation, and Experiment. *Progress in Aerospace Sciences*, 40(4-5): 237-289, 2004.

[8] Greenblatt, D. and Wignanski, I. J. The Control of Flow Separation by Periodic Excitation. *Progress in Aerospace Sciences*, 36(7): 487-545, 2000.

[9] Lin, J. C. Review of Research on Low-Profile Vortex Generators to Control Boundary-Layer Separation. *Progress in Aerospace Science*, 38(4-5) 389-420, 2002.

[10] Godard, G. and Stanislas, M. Control of a Decelerating Boundary Layer. Parts 1-3. *Aerospace Science and Technology*, 10(3, 5, 6): 181-191, 394-400, 455-464, 2006.

[11] Ekaterinaris, J. A. Predictions of Performance with Active Flow Control on Airfoils and Wings. *Journal of Aerospace Science and Technology*, 8(1): 401-410, 2004.

[12] Ekaterinaris, J. A. Numerical Investigation of Dynamic Stall Active Control of Incompressible and Compressible Flows. *Journal of Aircraft*, 39(1): 71-78, 2002.

[13] Brunet, V., Francois, C., Garnier, E., and Pruvost, M. Experimental and Numerical Investigations of Vortex Generator Effects. *AIAA Paper*, 2006-3027, 2006.

[14] Bak, C., Fuglsang, P., Johansen, J., and Antoniou, I. Wind Tunnel Tests of the NACA 63-415 and Modified NACA 63-415 Airfoil. RISOE National Laboratory, Denmark, RISOE Technical Report, R-1193 (EN), Dec. 2000.

[15] Spalart, P. R. and Allmaras, S. R. A One-Equation Turbulence Model for Aerodynamic Flows. AIAA Paper 1992 - 0439, 1992.

[16] Jameson, A. Aerodynamic Shape Optimization Using the Adjoint Method. Lecture Series, Von Karman Institute for Fluid Dynamics, Brussels, Belgium, Feb. 2003.